Dalton Transactions

Accepted Manuscript

ROYAL SOCIETY OF CHEMISTRY

www.rsc.org/dalton

Synthesis and characterization of novel niccolite metal formate frameworks $[(CH_3)_2NH_2][Fe^{III}M^{II}(HCOO)_6]$ (M^{II}=Zn, Ni, Cu)

Aneta Ciupa, Mirosław Mączka,* Anna Gągor, Adam Pikul, and Maciej Ptak

ABSTRACT

We report synthesis, X-ray diffraction, thermal, magnetic, Raman and IR studies of three heterometallic MOFs, $[(CH_3)_2NH_2][Fe^{III}M^{II}(HCOO)_6]$ with M=Zn (DMFeZn), Ni (DMFeNi) and Cu (DMFeCu), crystallizing in the niccolite type structure. DMFeZn and DMFeNi crystallize in the trigonal structure (space group $P\bar{3}1c$) while DMFeCu crystallizes in the monoclinic structure (space group $C2/c$). Magnetic investigation shows that DMFeZn remains paramagnetic down to the lowest temperature obtained in our experiment while DMFeNi and DMFeCu exhibit ferromagnetic order below 42 and 28.5 K, respectively. IR and Raman data confirm the structural model of the monoclinic DMFeCu and show evidence for stronger hydrogen bonds when compared to trigonal DMFeZn and DMFeNi. A different hydrogen bond network in the monoclinic DMFeCu when compared to trigonal DMFeZn and DMFeNi is responsible for different behavior of these compounds upon cooling, that is, DMFeCu exhibits a sign of short range ordering of dimethylaminium cations at low temperatures while the trigonal analogues show evolution of dynamic disorder into static disorder.

Introduction

Metal-organic frameworks (MOFs) are porous materials made up of metal ions connected by organic ligands forming extended flexible structures. Recently, a lot of attention was focused on the metal formate frameworks as potential ferroelectrics or multiferroics.[1-12] Some of these compounds were also shown to possess good gas sorption and luminescent properties.[13,14]

Compounds with the perovskite architecture of general formula $[(CH_3)_2NH_2][M(HCOO)_3]$ (M=Mg, Zn, Mn, Ni, Co, Fe) are well-known examples of MOFs exhibiting a paraelectric to ferroelectric phase transition at 160-260K and the long-range ferromagnetic ordering at 8-36K.[1,4-8,10,15] A structural phase transition was also discovered in another perovskite MOF, i.e., a heterometallic $[(CH_3)_2NH_2][Na_{0.5}Fe_{0.5}(HCOO)_3]$.[16] It is commonly accepted that the driving force for the observed structural changes in this family of compounds is ordering of dimethylammonium (DMA^+) cations located in the cavities of the framework.[1,4-8,10,15,16]

In the past few years, different formate-based framework topologies have been reported depending on the size of the used amine cations.[8] For example, employing larger linear amine such as N,N'-dimethylethylenediamine leads to formation of $[CH_3NH_2(CH_2)_2NH_2CH_3][M_2(HCOO)_6]$ (M=Mn, Fe, Co, Ni, Cu, Zn) frameworks with the niccolite architecture.[17,18] The anionic structure of these compounds contains metal-oxygen octahedra connected by $HCOO^-$ ligands in *anti-anti* mode of coordination.[17,18] The organic cations are located in the cavities of the framework. These cations are trigonally disordered, except of the Cu compound.[17,18]

The niccolite topology was also reported for mixed-valence and heterometallic MOFs containing DMA^+ cations with general formula $[(CH_3)_2NH_2][Fe^{III}M^{II}(HCOO)_6]$ (M^{II}=Fe, Co, Mn, Mg).[19-22] These compounds crystallize in a trigonal space group $P\bar{3}1c$.[19-22] An order-disorder phase transition into an antiferroelectric $R\bar{3}c$ phase was found for the mixed-valence $[(CH_3)_2NH_2][Fe^{III}Fe^{II}(HCOO)_6]$ only.[21,22] We have argued that this behavior can be related to the electronic contribution to the phase transition mechanism in this compound.[22]

Herein, we report the synthesis as well as structural, magnetic and vibrational properties of three novel heterometallic metal formate frameworks: DMFeZn, DMFeNi and DMFeCu. We will show that they crystallize in the niccolite topologies. However, whereas DMFeZn and DMFeNi crystallize in the trigonal structure (space group $P\bar{3}1c$), the structure of DMFeCu is monoclinic.

Experimental

Materials and instrumentation

All reagents (analytically grade) used for synthesis are commercially available and used without further purification. Elemental analysis (C, H, N) was performed on a Elementar Vario EL CHNS analyzer. The content of metal elements was determined by inductively coupled plasma method (ICP), which was performed on a ARL 3410 ICP instrument. The DSC measurements were performed on a DSC-7 instrument (Perkin Elmer) at a rate of 15 °C/min under a nitrogen atmosphere with two cycles. Freshly powdered samples were used. Magnetization of a large number of freely oriented tiny single crystals of DMFeNi, DMFeCu and DMFeZn was measured using a commercial superconducting quantum interference device (SQUID) magnetometer in the temperature range 2−80 K and in external magnetic fields up to 20 kOe. The background coming

from a weakly diamagnetic sample holder (not shown here) was found to be negligible when compared to the total signal measured. Therefore its subtraction was omitted. No demagnetization corrections were also made to the data reported here. The powder diffraction data were collected using X'Pert PRO X-ray diffraction system equipped with PIXcel ultra-fast line detector and Soller slits for *Cu* K_α radiation. The samples were measured in a reflection mode using the Bragg-Brentano geometry. Single-crystal XRD data were collected for DMFeNi using KM4-CCD diffractometer operating in κ-geometry and equipped with a two-dimensional CCD detector. *Mo Kα* radiation (0.71073Å) was used. IR spectra were measured using Biorad 575C FT-IR spectrometer for the sample in KBr pellet (spectral range 3800-400 cm^{-1}) or in Apiezon N suspension (spectral range 500-50 cm^{-1}). Raman spectra were measured using a Renishaw InVia Raman spectrometer equipped with confocal DM 2500 Leica optical microscope, a thermoelectrically cooled CCD as a detector and an argon laser operating at 488 nm. The spectral resolution of IR and Raman spectra was 2 cm^{-1}.

Synthesis of the sample

The three compounds were prepared under solvothermal conditions. All starting materials were commercially available and used without further purification. In order to synthesize DMFeNi, a mixture of HCOOH (30 ml), N,N-dimethylformamide (30 ml), $Fe(NO_3)_3 \cdot 9\ H_2O$ (1.5 mmol) and $NiCl_2$ (1.5 mmol) was heated in a Teflon-lined autoclave at 140°C for 24h. Small green crystals were collected after overnight cooling, washed by methanol and dried at room temperature. Anal. Calcd for DMFeNi (%): C, 22.31; H, 3.28; N, 3.25; Fe, 12.96; Ni, 13.63; Found (%): C, 22.04; H, 3.18; N, 3.16. ICP: Fe, 13.04; Ni, 13.92. Ratio of Fe:Ni=1:1.02. The same synthesis procedure with $ZnCl_2$ resulted in transparent solution without any precipitate. DMFeZn was collected after 10 days of crystallization from the solution, washed by methanol

and dried at room temperature. Anal. Calcd for DMFeZn (%): C, 21.97; H, 3.23; N, 3.20; Fe, 12.77; Zn, 14.94; Found (%): C, 21.94; H, 3.26; N, 3.15. ICP: Fe, 12.59; Zn, 14.40. Ratio of Fe:Zn=1.00:0.98.

The synthesis of DMFeCu needed different chemical composition of the mixture due to oxidation-reduction properties of the used compounds. In this case, we applied a solution composed of DMF (30 ml), HCOOH (10 ml), water (20 ml), $CuCl_2$ (2 mmol) and $FeCl_3$ (3 mmol). After reaction in the autoclave, brown precipitate was filtered off and the remaining transparent solution was left at room temperature undisturbed. Green DMFeCu crystals were collected after 5 days of crystallization. Yield of DMFeZn and DMFeCu was about 60~65% based on the Zn or Cu salt used. In case of DMFeNi, the yield was about 30 %. Anal. Calcd for DMFeCu (%): C, 22.06; H, 3.24; N, 3.22; Fe, 12.82; Cu, 14.59; Found (%): C, 22.14; H, 3.22; N, 3.19. ICP: Fe, 12.58; Cu, 14.50. Ratio of Fe:Cu=1.00:1.01.

Crystallographic Structure Determination

Single crystal data for DMFeNi were collected in ω-scan mode with $\Delta\omega$=1.0^o and processed using CrysAlisPro software.[23] The structure was solved by direct methods and refined using full-matrix least-squares method with SHELXL-2014/7.[24] Empirical absorption correction using spherical harmonics was applied on all data. The geometrical parameter restraints (DFIX) were used to fix disordered DMA^+ cations to be chemically reasonable. Hydrogen atoms were placed in calculated positions and refined as riding atoms. Profile matching and Rietveld refinement for the powder diffraction data for DMFeCu were done using Jana2006.[25]

Results and discussion

Crystal structure

The crystal structures of DMFeNi and DMFeZn are isomorphic to DMFeMg niccolite reported by us previously.[22] The details of data collection, cell, and refinement parameters for DMFeNi are summarized in Table S1. Tables S2 and S3 present details for bond lengths and angles as well as hydrogen bond geometry for DMFeNi. The single-crystal X-ray diffraction data measured for DMFeNi confirm trigonal crystal system and $P\bar{3}1c$ space group (Table S1). The DMA^+ counterions are arranged over 6 possible sites. Disorder affects also the metal formate framework since the best refinement results are obtained for Ni^{2+} and Fe^{3+} statistically distributed over the metal sites, with equal probability. Almost uniform metal-oxygen distances that are equal to 2.029(3)Å for metal at D_3 site (1/3, 2/3, 1/4) and 2.023(3) Å for metal at D_{6d} site (0, 0, 0) (Table S2) also confirm the proposed model. The single-crystal X-ray diffraction data were not available for DMFeZn because of too small size of the crystallites. Therefore, the powder diffraction study has been performed. Figure S1 shows diffractograms of DMFeNi and DMFeZn powders together with positions and relative intensity of diffraction patterns calculated for DMFeNi structure. The unit cell parameters obtained from the least squares fit through the angular differences between measured and indexed reflections are: a=8.184(1) Å, c=13.655(5) Å for DMFeNi and a=8.218(2) Å, c=13.748(8) Å for DMFeZn.

DMFeCu crystallizes in a form of heavily twinned rhomboidal prisms and has diffraction pattern considerably different than DMFeNi and DMFeZn analogues. In order to reveal the crystal structure the X-ray powder diffraction study has been performed on powdered crystals. The diffraction pattern for DMFeCu has been indexed in the monoclinic system with the unit cell parameters: a=8.3771(8)Å, b=14.095(2) Å, c=13.635(2), and β=92.96(6)° (Table S4). As the metric of the unit cell corresponds to the monoclinic cell with $C/2c$ space group reported for $C_{10}H_{20}Cu_2N_2O_2$ single crystals, the model from Kurmoo *et al.*[18] has been applied to the Rietveld refinement. All diffraction peaks were consistent with the $C2/c$ space group; however, the

differences between the two structures occurred to be too large to give even the approximated solution. In searching for the proper model the structural data of DMFeMg has been used. For the group $P\bar{3}1c$ there are 3 different subgroups isomorphic to $C2/c$. One of them transforms the hexagonal unit cell into the monoclinic one by (-1 1 0, 1 -1 0, 0 0 1) matrix.[26] In the case of DMFeMg the transformation gives the unit cell parameters a=8.22 Å, b=14.23 Å, c=13.88 Å and β~90° that are closely related to the experimentally found metric for DMFeCu powder. Using DMFeMg crystal structure and TRANSTRU program[27] the positions of all atoms have been transformed from the trigonal $P\bar{3}1c$ space group to the $C2/c$ mononoclinic structure and were used as a starting model for the Rietveld refinement. The results of the refinement are presented in Figure 1. The fit of the calculated to the observed structure factors is rather poor, although it evidences the proper assignment of the cell and symmetry, and the obtained structural model, illustrated in Figure 2, gives reasonable bond lengths and packing. During the course of the refinement a number of constraints on the M-O lengths and O-M-O angles have been applied to keep the bonds and angles in a range acceptable for Cu-O and Fe-O distances.

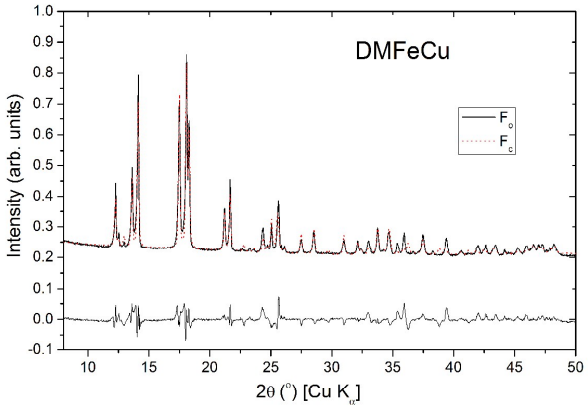

Figure 1. The results of the Rietveld refinement for DMFeCu: space group $C2/c$, a=8.377(1) Å, b=14.095(2) Å, c=13.635(2) Å, β=92.97(6); R_p=0.023, wR_p=0.035, R_1=0.11, wR_1=0.12.

In the monoclinic $C2/c$ structure Cu^{2+} and Fe^{3+} occupy C_2 and C_i symmetry site, respectively. The coordination spheres of both ions are distorted octahedra. The distances for Cu-O range from 2.08(3) Å to 2.19(3) Å and Fe-O bond lengths vary from 1.90(3) Å to 2.08(3) Å (Table S5). The DMA^+ counterions are disordered through at least two nonequivalent sites of C_2 symmetry. In the trigonal, nicollite structure, the DMA^+ are statistically distributed over six equivalent sites. Figure 2 illustrates the metal coordination spheres together with the crystal packing. The monoclinic c direction corresponds to the trigonal c axis (in hexagonal setting). The monoclinic distortion affects the spatial arrangement of metal polyhedra, induces their considerable rotation and loss of 3-fold symmetry. Figure 2 (d) presents ideal niccollite like arrangement of the polyhedra in $P\bar{3}1c$ symmetry, for comparison.

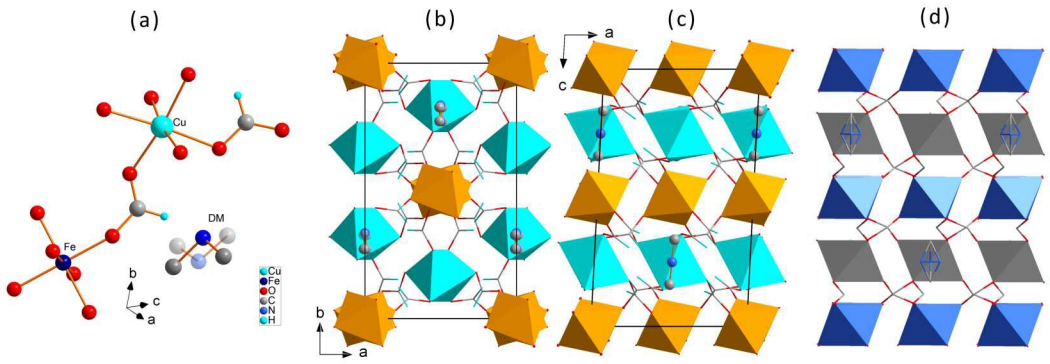

Figure 2. Crystal structure of DMFeCu; (a) coordination of the metal ions and possible model of disorder for DMA^+ counterions (b) pseudohexagonal arrangement of metal polyhedra, $c_{mono}=c_{hex}$; (c) two sublattices of the two types of metal ions in monoclinic DMFeCu, orange polyhedra stand for FeO_6; blue for CuO_6; (d) the related view of the DMFeNi in the trigonal symmetry.

Magnetic Properties

Figure 3 displays temperature dependence of the magnetization M of DMFeNi measured in an external magnetic field H of 100 Oe. An abrupt increase of M curve suggests that the compound is magnetically ordered below 42(2) K. Brilllouin-like shape of the anomaly and large difference between the data collected in zero-field- cooling (ZFC) and field-cooling (FC) regimes suggest ferromagnetic character of the ordering. Hysteresis observed in $M(H)$ up to about 10 kOe (see the inset to Figure 3) corroborates the latter hypothesis.

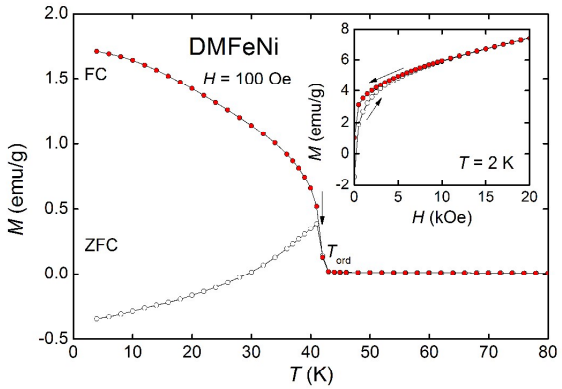

Figure 3. Temperature variation of magnetization M of DMFeNi measured in ZFC and FC regimes in steady external magnetic field H; solid lines serve as guides for the eye and the arrow marks the ordering temperature T_{ord}. Inset: M vs. H measured at constant temperature upon increasing and decreasing field (open and closed symbols, respectively); solid lines and arrows serve as guides for the eye.

DMFeCu exhibits very similar magnetic behavior. As can be inferred from Figure 4, it orders magnetically below about 28.5(5) K. Distinct bifurcation of the ZFC/FC curves and hysteresis in the $M(H)$ curve indicate that also this compound is a ferromagnet. It is worth noting that lower value of T_{ord} in DMFeCu is associated with smaller hysteresis loop – it is hardly visible already in 1 kOe (see the inset to Figure 4).

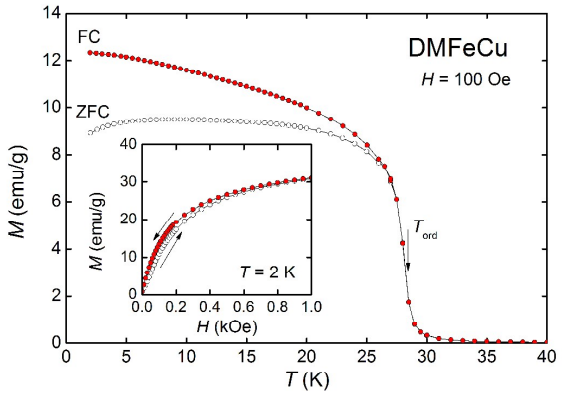

Figure 4. Magnetization of DMFeCu as a function of temperature measured in ZFC and FC regimes; solid lines serve as guides for the eye and the arrow marks the ordering temperature T_{ord}. Inset: field dependence of M measured upon increasing and decreasing field (open and closed symbols, respectively); solid lines and arrows serve as guides for the eye.

In contrast to DMFeNi and DMFeCu, the Zn-based compound remains paramagnetic down to the lowest temperature studied, as evidenced by nearly linear increase of the magnetization with increasing magnetic field and lack of any hysteresis loop in $M(H)$ (Figure S2).

The magnetic behavior observed in the DMFeNi and DMFeCu compounds is reminiscent of weak ferromagnetism, which is observed in many structurally related metal-organic frameworks.[20,28-31] The origin of the latter phenomena is an antisymmetric exchange or single-ion anisotropy,[32,33] which are very likely in the studied compounds. They often lead to a small canting of the spins in the underlying antiferromagnetic lattice and then result in a small ferromagnetic component of the moments, which is produced perpendicular to the spin-axis of the antiferromagnet.

It is worth noting that studies of $[CH_3NH_2(CH_2)_2NH_2CH_3][M_2(HCOO)_6]$ niccolites showed magnetic ordering at 8.6 K for Mn, 16.4 K for Co, 19.8 K for Fe and 33.7 K for Ni.[18] On the other hand, magnetic studies of $[(CH_3)_2NH_2][Fe^{III}M^{II}(HCOO)_6]$ (M^{II}=Fe, Co, Mn) revealed

magnetic ordering at significantly higher temperatures, i.e., 32, 35 and 37 K for Co, Mn and Fe members.[20] Our present studies show that the ordering temperature of DMFeNi (42 K) is also significantly higher that that observed for $[CH_3NH_2(CH_2)_2NH_2CH_3][Ni_2(HCOO)_6]$. Interestingly, DMFeCu orders at 28.5 K although no ordering was observed for $[CH_3NH_2(CH_2)_2NH_2CH_3][Cu_2(HCOO)_6]$ niccolite.[18] This behaviour proves that presence of Fe^{3+} magnetic sub-lattice leads to significant increase of the ordering temperature and reported here DMFeNi has the highest T_{ord} among the reported so far in literature amine-templated metal formate frameworks.

Vibrational properties at room temperature

The observed Raman and IR bands should be assigned to internal vibrations and librations of the DMA^+ and formate ions as well as translational motions of these ions and metal cations. There are six internal modes for the free $HCOO^-$ ion of C_{2v} symmetry, namely the C-H stretching mode ν_1, the symmetric C-O stretching mode ν_2, the antisymmetric C-O stretching mode ν_4, the symmetric O-C-O bending mode ν_3, the C-H in-plane bending mode ν_5, and the C-H out-of-plane bending mode ν_6.[15,34,35] In case of DMA^+, the internal modes can be classified as symmetric stretching ($\nu_s(NH_2)$), antisymmetric stretching (($\nu_{as}(NH_2)$), scissoring ($\delta(NH_2)$), rocking ($\rho(NH_2)$), wagging ($\omega(NH_2)$) and torsion or twisting ($\tau(NH_2)$) modes of the NH_2 group; symmetric stretching ($\nu_s(CNC)$), antisymmetric stretching ($\nu_{as}(CNC)$) and bending ($\delta(CNC)$) modes of the CNC group; symmetric stretching ($\nu_s(CH_3)$), antisymmetric stretching (($\nu_{as}(CH_3)$), bending ($\delta(CH_3)$), rocking ($\rho(CH_3)$) and torsion ($\tau(CH_3)$) modes of the methyl groups.[10,15,34] Distribution of these vibrational modes among irreducible representations of D_{3d} (for DMFeZn

and DMFeNi) and C_{2h} (for DMFeCu) point groups is presented in Table S6. This table shows that the number of Raman- and IR-active vibrational modes of the *C*2/*c* structure should be larger than for the $P\bar{3}1c$ one. In particular, the doubly degenerate modes of DMFeZn and DMFeNi should split in DMFeCu due to monoclinic distortion and silent modes should become Raman- or IR-active. For instance, each internal mode of $HCOO^-$ ion should have 3 Raman-active and 3 IR-active modes in the trigonal phase but the number of these modes should double in the monoclinic phase (see Table S6).

The room temperature IR and Raman spectra of the studied compounds are presented in Figures. 5 and 6. The observed IR and Raman frequencies (in cm^{-1}) and the proposed assignments are listed in Table S7. The assignment of bands corresponding to internal vibrations could easily be done by comparison with the spectra of other related metal formates with dimethylammonium (DMA^+) because these modes appear in narrow wavenumber ranges.[10,14-16, 22, 34]

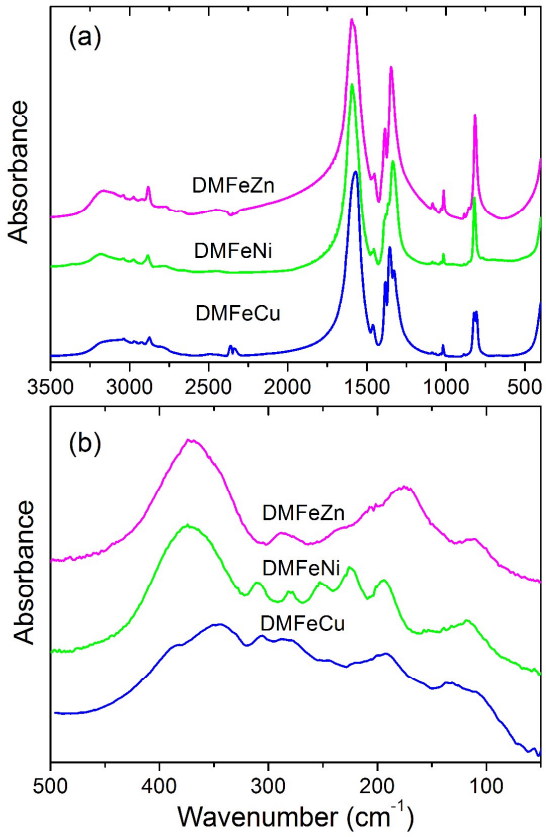

Figure 5. Room-temperature spectra of DMFeZn, DMFeNi and DMFeCu in the (a) mid-IR and (b) far-IR region.

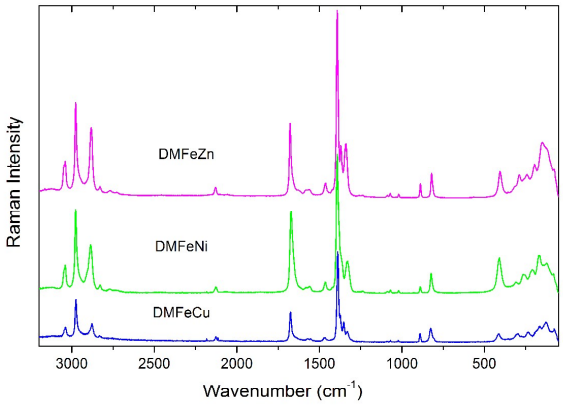

Figure 6. Room-temperature Raman spectra of DMFeZn, DMFeNi and DMFeCu.

The IR and Raman spectra of DMFeZn and DMFeNi corresponding to internal modes (above 700 cm^{-1}) are very similar. They are also very similar to the spectra of previously reported DMFeFe and DMFeMg.[22] In particular, the frequency difference between the same modes is only a few cm^{-1} for majority of modes (see Table S7). This behavior indicates that type of divalent cation has weak effect on vibrational properties of the studied niccolites. Nevertheless, it can be noticed that frequencies of the ν_1 and ν_3 modes are the highest for DMFeNi and this behavior can be attributed to significantly smaller ionic radius of Ni^{2+} when compared to Zn^{2+}, Fe^{2+} and Mg^{2+}. Our results also show that Raman and IR spectra of monoclinic DMFeCu are very similar to those recorded for trigonal DMFeZn, DMFeNi, DMFeFe and DMFeMg. However, the splitting of the ν_4 IR band is significantly larger for DMFeCu (20 cm^{-1}) than DMFeZn (13 cm^{-1}) and DMFeNi (10 cm^{-1}). Since this splitting reflects difference in the C-O bond lengths of the $HCOO^-$ ions,[14,16,22] larger splitting for DMFeCu suggests more distorted metal formate framework in this compound. This conclusion is consistent with X-ray data, which indicate the C-O bond lengths of 1.2077-1.3193 Å for DMFeCu and 1.231-1.244 Å for DMFeNi. Stronger distortion of the metal formate framework in DMFeCu is further supported by observation of additional bands for the ν_2 Raman-active and ν_3 IR-active modes (three components for monoclinic DMFeCu and only two for the remaining trigonal compounds, see Table S7 and Ref. 22). It worth adding that although majority of internal modes of DMFeCu are observed in a very similar wavenumber range as the corresponding modes in trigonal niccolites, there is one interesting exception, that is, the $\rho(NH_2)$ mode. This mode is observed in all trigonal compounds near 852-855 cm^{-1} (see Table S7 and [22]). This mode is not well visible for DMFeCu at room temperature but our low-temperature studies (see next paragraph) clearly indicate that it is overlapped by the ν_s(CNC) band, i.e., it is observed near 880 cm^{-1}. Such significant shift towards higher wavenumbers points to significant

difference in strength of the hydrogen bonds in the monoclinic and trigonal niccolites. A comparison of the data shows that this band has quite similar wavenumber as the bands observed in [DMA][$M(HCOO)_3$] perovskites,[10,15,34] which present stronger hydrogen bonds when compared to niccolites.[22] Our IR data indicate, therefore, that monoclinic DMFeCu has stronger hydrogen bonds when compared to trigonal niccolites. It is worth noting that this observation supports the structural model of DMFeCu. Namely, the shortest N···O distance within the N-H···O hydrogen bond is significantly shorter in DMFeCu (2.81 Å) than in DMFeNi (3.01 Å).

In contrast to the internal modes, the Raman and IR spectra show much larger differences in the lattice modes region (below 500 cm^{-1}). It is well known that wavenumbers of the lattice modes should depend significantly on mass and size of ions building the structure. Firstly, the wavenumber of a translational mode should be approximately proportional to the square root of the appropriate reciprocal reduced mass.[36] Since the atomic masses of Zn (65.4), Cu (63.5) and Ni (58.7) are quite similar, the mentioned above rule predicts that translational modes of divalent cations should differ by no more than 6 %. Secondly, the translational modes should shift to higher wavenumbers with decreasing ionic size of M^{2+} due to decrease of the unit cell volume. Since the ionic radius of Zn^{2+} (0.88 Å) is nearly the same as the ionic radius of Cu^{2+} (0.87 Å),[37] this effect should be negligible for these cations. Some shift towards higher wavenumbers can be, however, expected for DMFeNi due to smaller size of Ni^{2+} (0.83 Å).[37] Based on previous studies of metal formates we assign the intense IR bands at 345-372 cm^{-1} to translations of both Fe^{3+} and divalent M^{2+} cations.[14,16,22] These bands are observed at nearly the same wavenumbers for isostructural DMFeNi and DMFeZn (371-372 cm^{-1}), in agreement with the expected weak dependence of T'(M^{2+}) modes on type of the divalent cation. It can be noticed, however, that the monoclinic distortion of the copper formate framework is clearly evidenced through splitting of the corresponding band in DMFeCu into two components at 345 and 384 cm^{-1}. The large

splitting is consistent with large distortion of the CuO_6 octahedra. Other expected lattice modes are translational and librational modes of $HCOO^-$ and DMA^+ ions. Our previous studies showed that the low-wavenumber Raman (IR) spectra of formates are dominated by bands corresponding to librations (translations) of the $HCOO^-$ ions.[9,10,12,15,35] Lattice modes of DMA^+ cations were shown to contribute to the bands below 170 cm^{-1}.[10,15,34] We assign, therefore, the 200-315 cm^{-1} bands to translational motions of $HCOO^-$ and those below 200 cm^{-1} to librations of the $HCOO^-$ ions.

Temperature-dependent IR Studies

Although our DSC studies have not shown presence of any structural phase transitions in the studied compounds above 105 K (see Figure S3), we have decided to measure IR spectra down to 5 K in order to obtain further insight into properties of these niccolites. Some representative spectra are shown in Figures S4-S6 and Figure 7.

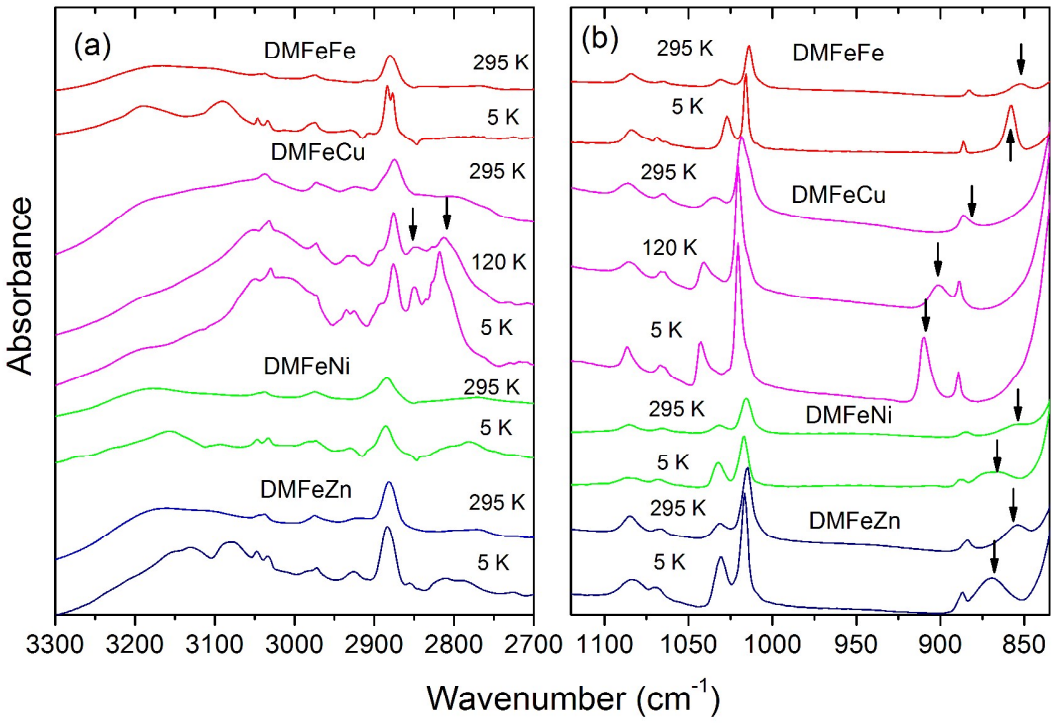

Figure 7. Comparison of the room temperature and low temperature IR spectra of DMFeZn, DMFeNi and DMFeCu in the (a) 3300-2700 and (b) 1120-835 cm^{-1} range showing different behavior of trigonal (DMFeZn and DMFeNi) and monoclinic (DMFeCu) niccolites. For the comparison sake, IR data for previously reported DMFeFe,[22] are also presented. Arrows indicate (a) the N-H stretching and (b) $\rho(NH_2)$ modes that exhibit strong increase in intensity and narrowing upon cooling.

These figures show that the bands corresponding to internal modes of $HCOO^-$ do not exhibit any splitting or significant change in relative intensities upon cooling, confirming the absence of any structural phase transition down to 5 K. This conclusion is further supported by lack of any anomalies in plots of frequency and full width at half maximum (FWHM) shown for a few modes in Figures 8, S7 and S8. It can be noticed that behavior of DMFeNi and DMFeZn is very

similar to that observed previously for DMFeMg,[22] i.e. the band corresponding to the $\rho(NH_2)$ mode exhibits significant shift upon cooling but its FWHM changes weakly (see Figures 7 and 8). Thus similarly as in DMFeMg, the dynamic disorder of DMA^+ cations evolves on cooling into static disorder. Interestingly, DMFeCu shows very different behavior. Firstly, the $\rho(NH_2)$ mode exhibits pronounced narrowing upon cooling (Figures 7 and 8). As a result, its FWHM at 5 K (6.0 cm^{-1})) is comparable to the FWHM observed in a well ordered DMFeFe niccolite (6.5 cm^{-1},[22]) or $[DMA][M(HCOO)_3]$ perovskites (4.4, 5.0 and 4.4 cm^{-1} for M=Mn, Ni and Fe, respectively[10,15]). Secondly, the bands at 2804 and 2838 cm^{-1} exhibit strong narrowing and increase in intensity upon cooling. This behavior is very similar to that observed for $[DMA][M(HCOO)_3]$ perovskites, which showed pronounced increase in intensity of a band near 2800 cm^{-1},[10,15] and $[NH_4][M(HCOO)_3]$ chiral frameworks, which also showed increased intensity of a band near 2840-2860 cm^{-1} due to ordering of NH_4^+ cations.[9,35] Our results indicate, therefore, that in contrast to DMFeMg, DMFeZn and DMFeNi, the DMA^+ cations in DMFeCu exhibit a sign of short range ordering at low temperatures.

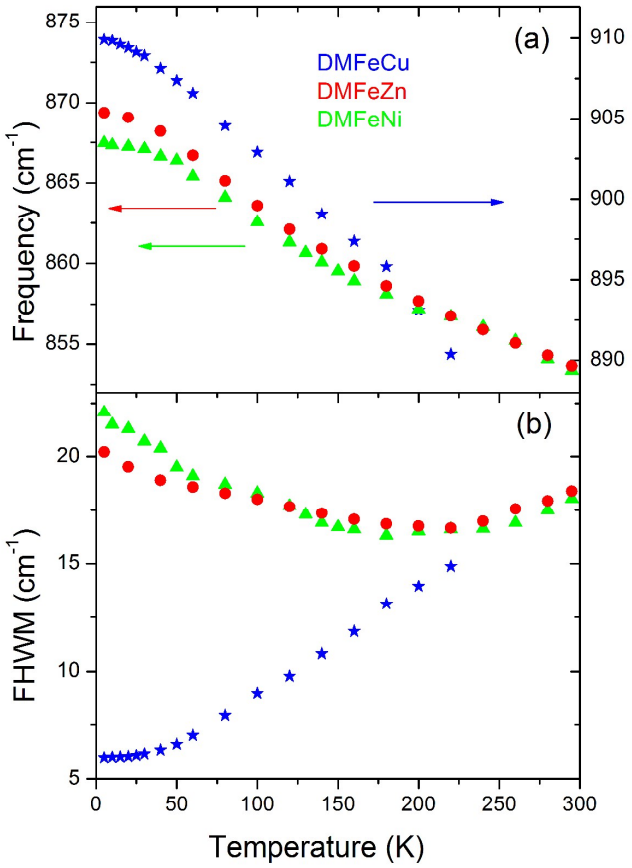

Figure 8. (a) Temperature dependence of the $\rho(NH_2)$ IR frequencies and (b) the corresponding FWHM values for DMFeZn, DMFeNi and DMFeCu. Significant increase of FWHM for DMFeCu is evident even at temperatures smaller than 100 K.

Figures 8, S7 and S8 also show that there are no anomalies in the temperature dependence of phonon modes near magnetic transitions, although clear anomalies were observed for DMFeFe.[22] This result confirms that DMFeFe is unique in this niccolite family since only this compound exhibits structural phase transitions and anomalies near magnetic ordering temperature. Thus our present results further supports the conclusion that different behavior of mixed-valence DMFeFe may be related to its electronic properties and change of the rate of electron transfer with decreasing temperature.

Conclusions

We have synthesized three novel heterometallic MOFs, $[(CH_3)_2NH_2][Fe^{III}M^{II}(HCOO)_6]$ with M=Zn, Ni and Cu, crystallizing in the niccolite type structure. X-ray diffraction studies revealed that DMFeZn and DMFeNi crystallize in the trigonal structure (space group $P\bar{3}1c$) whereas DMFeCu has monoclinic structure ($C2/c$), with strongly distorted CuO_6 octahedra due to the Jahn-Teller effect of the Cu^{2+} ion. Low-temperature magnetic studies show that DMFeNi exhibits ferromagnetic ordering below 42(2) K and this ordering temperature is the highest among amine-templated metal formate framreworks.

We also studied our compounds using Raman and IR spectroscopic methods. These methods were especially useful in studies of DMFeCu since due to lack of single-crystal X-ray diffraction data, the structural model could be proposed only on base of powder X-ray diffraction studies. Therefore, Raman and IR studies play important role in understanding structural properties of this compound and its behavior upon cooling. The obtained by us data confirmed lower symmetry of DMFeCu when compared to DMFeM (M=Zn, Ni, Fe and Mg). However, the observed differences in the vibrational spectra above 1000 cm^{-1} are small suggesting that the structure of the $HCOO^-$ ions is weakly affected by symmetry lowering. This is consistent with X-ray diffraction data showing that the major distortion of the structure is related to CuO_6 octahedra. Our IR data give also evidence for stronger hydrogen bonds in monoclinic DMFeCu when compared to trigonal DMFeZn and DMFeNi, and this observation supports the structural model of DMFeCu. Finally, our data give evidence for some short range ordering of DMA^+ cations at low temperatures for DMFeCu and lack of any ordering for DMFeZn and DMFeNi.

Acknowledgements

This research was supported by the National Center for Science (NCN) in Poland under project No. DEC-2013/11/B/ST5/01058.

Notes

Institute of Low Temperature and Structure Research, Polish Academy of Sciences, Box 1410, 50-950 Wrocław 2, Poland; m.maczka@int.pan.wroc.pl; phone: +48-713954161; fax: +48-713441029

Electronic Supplementary Information (ESI) available: X-ray crystallographic information files (CIF) for crystal structures of DMFeNi and DMFeCu. Figures S1-S8: Powder X-ray diffraction, magnetization, DSC traces, IR and Raman spectra, temperature dependence of bandwidths and frequencies. Tables S1-S7: data collection and refinement parameters, bond lengths and angles, hydrogen bond geometry for DMFeNi and DMFeCu, the correlation diagram showing number of expected vibrational modes for DMFeZn, DMFeNi and DMFeCu, and Raman and IR frequencies for all samples at room temperature.

References

1 P. Jain, V. Ramachandran, R. J. Clark, H. D. Zhou, B. H. Toby, N. S. Dalal, H. W. Kroto, A. K. J. Cheetham, *J. Am. Chem. Soc*., 2009, **131**, 13625.

2 G. C. Xu, W. Zhang, X. M. Ma, Y. H. Hen, L. Zhang, H. L. Cai, Z. M. Wang, R. G. Xiong, S. J. Gao, *J. Am. Chem. Soc*., 2011, **133**, 14948.

3 D. W. Fu, W. Zhang, H. L. Cai, Y. Zhang, J. Z. Ge, R. G. Xiong, S. D. Huang, T. Nakamura, *Angew. Chem. Int. Ed*., 2011, **50**, 11947.

4 G. Rogez, N. Viart, M. Drillon, *Angew. Chem. Int. Ed.* 2010, **49,** 1510.

5 Y. Tian, A. Stroppa, Y. Chai, L. Yan, S. Wang, P. Barone, S. Picozzi, Y. Sun, *Sci. Rep.* 2014, **4,** 1.

6 T. Besara, P. Jain, N. S. Dalal, P. L. Kuhns, A. P. Reyes, H. W. Kroto, A. K. Cheetham, *J. Proc. Nat. Acad. Soc*., 2011, **108**, 6828.

7 P. Jain, N. S. Dalal, B. H. Toby, H. W. Kroto, A. K. Cheetman, *J. Am. Chem. Soc.* 2008, **130,** 10450.

8 R. Shang, S. Chen, Z. M. Wang, S. Gao, in *Metal-Organic Framework Materials*. Edited by R. L. MacGillivray and C. M. Lukehart., John Wiley & Sons Ltd., 2014, pp. 221-238.

9 M. Mączka, A. Pietraszko, B. Macalik, K. Hermanowicz, *Inorg. Chem*., 2014, **53**, 787.

10 M. Mączka, A. Gągor, B. Macalik, A. Pikul, M. Ptak, J. Hanuza, *Inorg. Chem*., 2014, **53**, 457.

11 M. Mączka, M. Ptak, S. Kojima, *Appl. Phys. Lett*., 2014, **104**, 222903.

12 M. Mączka, P. Kadłubański, P. T. C. Freire, B. Macalik, W. Paraguassu, K. Hermanowicz, J. Hanuza, *Inorg. Chem*., 2014, **53**, 9615.

13 A. Rossin, G. Giambiastiani, M. Peruzzini, R. Sessoli, *Inorg. Chem.* 2012, **51,** 6962.

14 M. Mączka, B. Bondzior, P. Dereń, A. Sieradzki, J. Trzmiel, A. Pietraszko, J. Hanuza, *Dalton Trans.*, 2015, **44,** 6871.

15 M. Mączka, M. Ptak, L. Macalik, *Vib. Spectrosc*., 2014, **71**, 98.

16 M. Mączka, A. Pietraszko, L. Macalik, A. Sieradzki, J. Trzmiel, A. Pikul, *Dalton Trans.* 2014, **43,** 17075.

17 Z. Wang, X. Zhang, S. R. Batten, M. Kurmoo, S. Gao, *Inorg. Chem.* 2007, **46,** 8439.

18 M.-Y. Li, M. Kurmoo, Z.-M. Wang, S. Gao, *Chem. Asian J*., 2011, **6**, 3084.

19 K. S. Hagen, S. G. Naik, B. H. Huynh, A. Masello, G. Christou, *J. Am. Chem. Soc*., 2009, **131**, 7516.

20 J.-P. Zhao, B.-W. Hu, F. Lloret, J. Tao, Q. Yang, X.-F. Zhang, X.-H. Bu, *Inorg. Chem*., 2010, **49**, 10390.

21 L. Cañadillas-Delgado, O. Fabelo, J. A. Rodríguez-Velamazán, M.-H. Lemėe-Cailleau, S. A. Mason, E. Pardo, F. Lloret, J.-P. Zhao, X.-H. Bu, V. Simonet, C. V. Colin, J. Rodríguez-Carvajal, *J. Am. Chem. Soc*., 2012, **134**, 19772.

22 A. Ciupa, M. Mączka, A. Gągor, A. Sieradzki, J. Trzmiel, A. Pikul, M. Ptak, *Dalton Trans.*, DOI: 10.1039/c5dt00512d.

23 CrysAlisPro, Oxford Diffraction Ltd., Version 1.171.33.42

24 G. M. Sheldrick, *Acta Cryst*. *A* 2008, **64,** 112.

25 V. Petricek, M. Dusek, L. Palatinus, *Z. Kristallogr*. 2014, **229,** 345.

26 S. Ivantchev, E. Kroumova, G. Madariaga, J. M. Perez-Mato, M. I. Aroyo, *J. Appl. Cryst.* 2000, **33,** 1190.

27 M. I. Aroyo, J. M. Perez-Mato, D. Orobengoa, E. Tasci, G. de la Flor, A. Kirov, "Crystallography online: Bilbao Crystallographic Server" Bulg. Chem. Commun. 2011, **43,** 183.

28 X.-Y. Wang, L. Gan, S.-W. Zhang, S. Gao, *Inorg. Chem*. 2004, **43,** 4615.

29 Z. Wang, B. Zhang, K. Inoue, H. Fujiwara, T. Otsuka, H. Kobayashi, M. Kurmoo, *Inorg. Chem*. 2007, **46,** 437.

30 G.-C. Xu, W. Zhang, X.-M. Ma, Y.-H. Chen, L. Zhang, H.-L. Cai, Z.-M. Wang, R.-G. Xiong, S. Gao, *J. Am. Chem. Soc*. 2011, **133,** 14948.

31 A. Ciupa, M. Mączka, A. Gągor, A. Pikul, E. Kucharska, J. Hanuza, A. Sieradzki, *Polyhedron* 2015, **85,** 137.

32 I. Dzyaloshinsky, *J. Phys. Chem. Solids* 1958, **4,** 241.

33 T. Moriya, *Phys. Rev*. 1960, **120,** 91.

34 M. Mączka, W. Zierkiewicz, D. Michalska, J. Hanuza, *Spectrochim. Acta A*., 2014, **128**, 674.

35 M. Mączka, K. Szymborska-Małek, A. Ciupa, J. Hanuza, *Vibr. Spectrosc.* 2015, **77,** 17.

36 M. Nicol, J. F. Durana, *J. Chem. Phys.* 1971, **54,** 1436.

37 R. D. Shannon, *Acta. Crystallogr. A* 1976, **32,** 751.

We report the synthesis, structural, magnetic, Raman and IR studies of novel niccolite-type heterometallic $[(CH_3)_2NH_2]Fe^{III}M^{II}(HCOO)_6]$ compounds (M^{II}=Ni, Zn and Cu). The Ni and Cu compounds order ferromagnetically at 42 and 28.5 K, respectively. Our data show that the monoclinic Cu member exhibits significantly different structural changes on cooling compared to the trigonal Zn and Ni compounds due to highly distorted metal-formate framework and different hydrogen bond network.